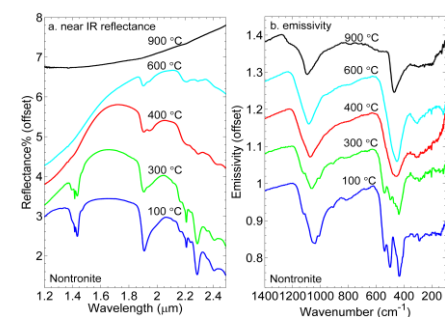


CHARACTERIZING DEHYDRATED AND DEHYDROXYLATED PHYLLOSILICATES ON MARS USING THERMAL AND NEAR IR SPECTROSCOPY. C. Che¹ and T. D. Glotch¹, ¹ Department of Geosciences, Stony Brook University, Stony Brook, NY 11794 (cche@ic.sunysb.edu)

Introduction: Phyllosilicates are detected in a number of contexts on Mars, primarily associated with ancient Noachian terrains [e.g., 1-4]. These phyllosilicate deposits may have been altered by multiple processes. We hypothesize that dehydrated and dehydroxylated phyllosilicates may be present on the Martian surface as one of the consequences of widespread impacts and volcanism during the Noachian and early Hesperian. In addition, thermal IR (TIR) and near IR (NIR) remote sensing data give different perspectives on phyllosilicate mineralogy, crystallinity, and abundance on Mars [e.g., 5-8]. Among the potential reasons for this disconnect is the possibility that phyllosilicates on Mars have been modified by the effects of dehydration and dehydroxylation. Such effects could modify the mineral structures in such a way that their spectroscopic signatures appear different from various wavelength perspectives, and different instruments.

Under our previously funded MFRP grant, we have acquired NIR reflectance and TIR emissivity spectra of a suite of 14 phyllosilicates (coming from four structural groups: kaolinite, smectite, chlorite, and palygorskite-sepiolite) and 2 natural zeolite minerals and their thermal decomposition products [9]. Results from this laboratory work show that phyllosilicates may lose all original spectral features in the TIR region while displaying familiar spectral bands of phyllosilicates in the NIR region in the same temperature range (Figures 1 and 2).



single absorption centered at $\sim 450 \text{ cm}^{-1}$, while the nontronite sample maintains weak 1.9, 2.3, and 2.4 μm spectral bands in NIR region.

The objective of this work is to identify, map, and characterize these dehydrated and dehydroxylated phyllosilicates on Mars, using TES and CRISM data. The significant suite of our previous laboratory spectra will be the basis for our TES and CRISM data analysis. The identification of these phases on Mars would help provide insights into the role of post-depositional thermal alteration of phyllosilicates-bearing sediments.

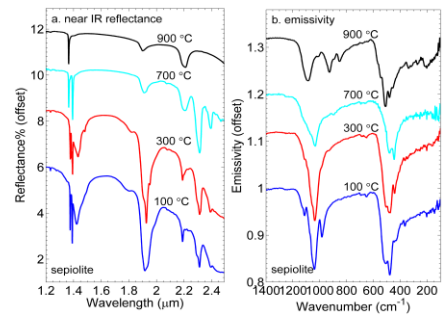


Figure 2. (a) Near IR reflectance and (b) TIR emissivity spectra of heated sepiolite. At 900 °C, sepiolite displays spectral bands at 1.9 and 2.2 μm that are diagnostic of

phyllosilicates, while its TIR spectrum is already dominated by spectral bands of enstatite.

Methods: We used a variety of spectroscopic methods, covering NIR to MIR wavelengths to map the distribution of dehydrated and dehydroxylated phyllosilicates on Mars. These include (1) global- and local-scale linear deconvolution of TES data using a spectral library that includes dehydrated and dehydroxylated phyllosilicates, (2) use of spectral ratios of TES data to determine the long-wavelength spectral character of phyllosilicate-bearing deposits, (3) global and local-scale spectral index mapping of dehydrated and dehydroxylated phyllosilicates, based on the unique TIR spectral properties of these phases, (4) factor analysis and target transformation (FATT) analyses of TES data, to determine the independently variable spectral components in regions of interest, and (5) spectral index mapping and detailed spectral analysis of CRISM data.

Here we present the preliminary results using the above methods, contributing to a better understanding of nontronites in the Nili Fossae region.

Preliminary Results: *Preliminary Study Region: Nili Fossae (Figure 3):* Michalski et al. [2010] [10] analyzed the nontronite deposits in the Nili Fossae region using TES data, but did not detect the spectral features showing the occurrences of nontronite in the long-wavelength region. Instead, TES data consistently exhibited a spectral absorption located near $\sim 450 \text{ cm}^{-1}$ on the same surface where OMEGA and CRISM data identified the diagnostic NIR spectral bands (1.9, 2.3, and 2.4 μm) of nontronite [10, 11]. This leads us to investigate whether nontronites in this region were affected by post-depositional thermal alteration.

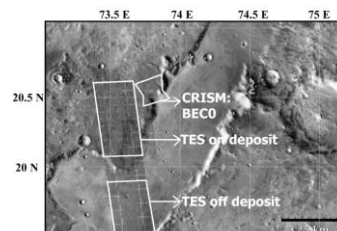


Figure 3. Context image of the Nili Fossae region showing positions of TES and CRISM data presented

below and shown in Figure 4, 6, and Table 1. The surface “on deposit” was determined to be nontronite-bearing based on CRISM and OMEGA data [10, 11], while the surface “off deposit” appears spectrally “neutral” in OMEGA data [10].

Local Deconvolution of TES spectra (Table 1): We deconvolved TES spectra of the surface “on deposit” and “off deposit” in Figure 3. We used a 49 endmember spectral library composed of a range of silicates, carbonate, sulfates, and oxides that also included spectra of thermally altered nontronite (at 400 °C) acquired by Che and Glotch [2011] [9].

Mineral Group	On Deposit	Off Deposit
Altered Nontronite	19±8	5±6
Pyroxene	27±5	30±4
Plagioclase	18±5	26±4
Sulfate	6±3	7±2
Carbonate	5±1	6±1
Olivine	10±3	7±3
Phyllosilicates	8±4	13±4
Other	6±3	6±2
RMS Error (%)	0.1473	0.1608

Table 1. Modeled mineral abundances of TES spectra of “on deposit” and “off deposit”. It appears that on deposit, the altered nontronite is largely substituting for the unaltered phyllosilicates and plagioclase.

Index Mapping of TES Data at Regional Scales (Figure 4): We created a 450 cm⁻¹ (spectral feature of 400 °C nontronite shown in Figure 1b) index map around Nili Fossae to identify small areas of interest.

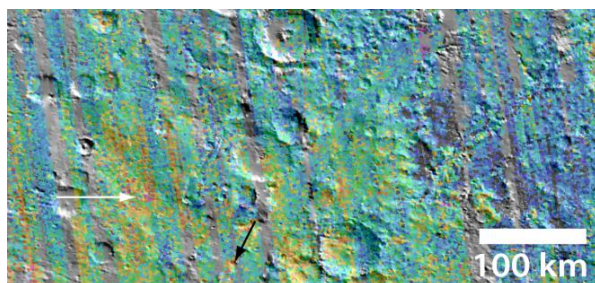
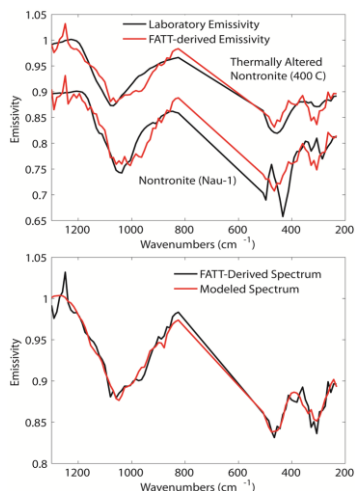


Figure 4: Regional-scale map of the 450 cm⁻¹ index in the Nili Fossae region. The black arrow points to a high index value that corresponds to the TES spectra outlined in Figure 3. Index mapping and deconvolution results (Table 1) both suggest the presence of thermally altered nontronite in Nili Fossae region.

FATT of TES Data (Figure 5 and Table 2): We gathered 5616 individual TES spectral from the region



shown in Figure 3. We used both our heated and unheated nontronite spectra as target vectors. FATT-derived spectral results are shown in Figure 5 and Table 2.

Figure 5: a) FATT-derived spectra of heated nontronite and unheated nontronite. b) Linear deconvolution of our FATT-derived spectrum of heated nontronite.

Mineral Group	Abundance
Altered Nontronite	46±6
Other Phyllosilicates	20±7
Olivine	8±4
Plagioclase	6±11
Amphibole	6±4
Pyroxene	5±6
Sulfate	4±2
Carbonate	4±1

Table 2. Modeled mineral abundances of our FATT-derived spectrum of heated nontronite.

The TES data provide a much better fit to the heated nontronite. This FATT-derived spectrum is modeled as 46% heated nontronite, 20% other phyllosilicates, and <10% of all other phases.

Detailed spectral index mapping of CRISM data (Figure 6): At 400 °C, nontronite loses its 1.4 μm band completely while it still keeps a strong 1.9 μm feature (Figure 1), therefore we mapped the ratio of the 1.4 to 1.9 μm band depth indices in CRISM images to gain insights into the degree of thermal alteration of nontronite-bearing surfaced on Mars.

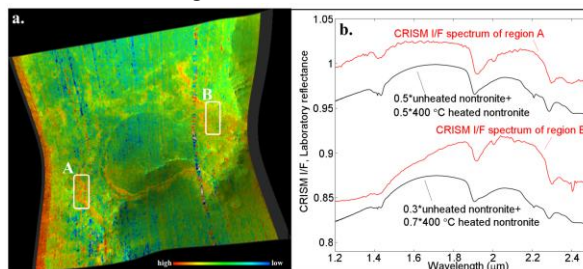


Figure 6. a) Ratio of 1.4 and 1.9 μm indices from CRISM image FRT0000BEC0 (Shown in Figure 3) overlaid on 1.3 μm reflectance. B) CRISM I/F spectra shown for each of the regions of interest and compared to spectra of mixtures of unheated and heated nontronite.

The spectrum of spot A displays a relatively higher 1.4/1.9 μm index value than spot B. One interpretation of this observation is that spot B has more thermally altered nontronite than spot A.

Summary and Future Work: Our preliminary results suggest the presence of thermally altered nontronite in Nili Fossae region. The results also suggest that mixing is occurring and the thermally altered nontronite may not exist as a pure phase on the surface. We will continue to use these spectroscopic methods to investigate the thermally altered phyllosilicates on Mars.

References: [1] Bibring J. -P. et al. (2006) *Science* 312, 400–404. [2] Loizeau D. et al (2007) *J. Geophys. Res.* 112, E08S08. doi:10.1029/2006JE002877. [3] Poulet F. et al. (2005) *Nature*, 438, 623–627. [4] Mangold N. et al. (2007) *J. Geophys. Res.* 112, E08S04. doi:10.1029/2006JE002835. [5] Bandfield J. L. (2002) *J. Geophys. Res.* 107(E6), 5042. doi:10.1029/2001JE001510. [6] Ruff S. W. (2003) *Intl. Conf. Mars* 6, 3258 (abstract). [7] Ruff S. W. and Christensen P. R. (2007) *Geophys. Res. Lett.* 34, L10204. doi: 10.1029/2007GL029602. [8] Michalski J. R. et al. (2006) *J. Geophys. Res.* 111, E03004. doi:10. 1029/2005JE002438. [9] Che C. and Glotch, T. D. (2011) *Icarus*, under review. [10] Michalski J. R. et al. (2010) *Icarus*, doi:10.1016/j.icarus.2009.09.006. [11] Ehlmann B. L et al (2009), *J. Geophys. Res.*, 114, E00D08, doi:10.1029/2009JE003339.